

Stochastic perturbations representing the mechanical effect of subgrid-scale orography

Fabian Brundke, Kirstin Kober, George C. Graig

Meteorologisches Institut, Ludwig-Maximilians Universität München (Fabian.Brundke@campus.lmu.de)

Diurnal cycle problem

Forecasting the diurnal cycle of precipitation in synoptic situations with weak large-scale forcing shows low skill in mesoscale NWP models:

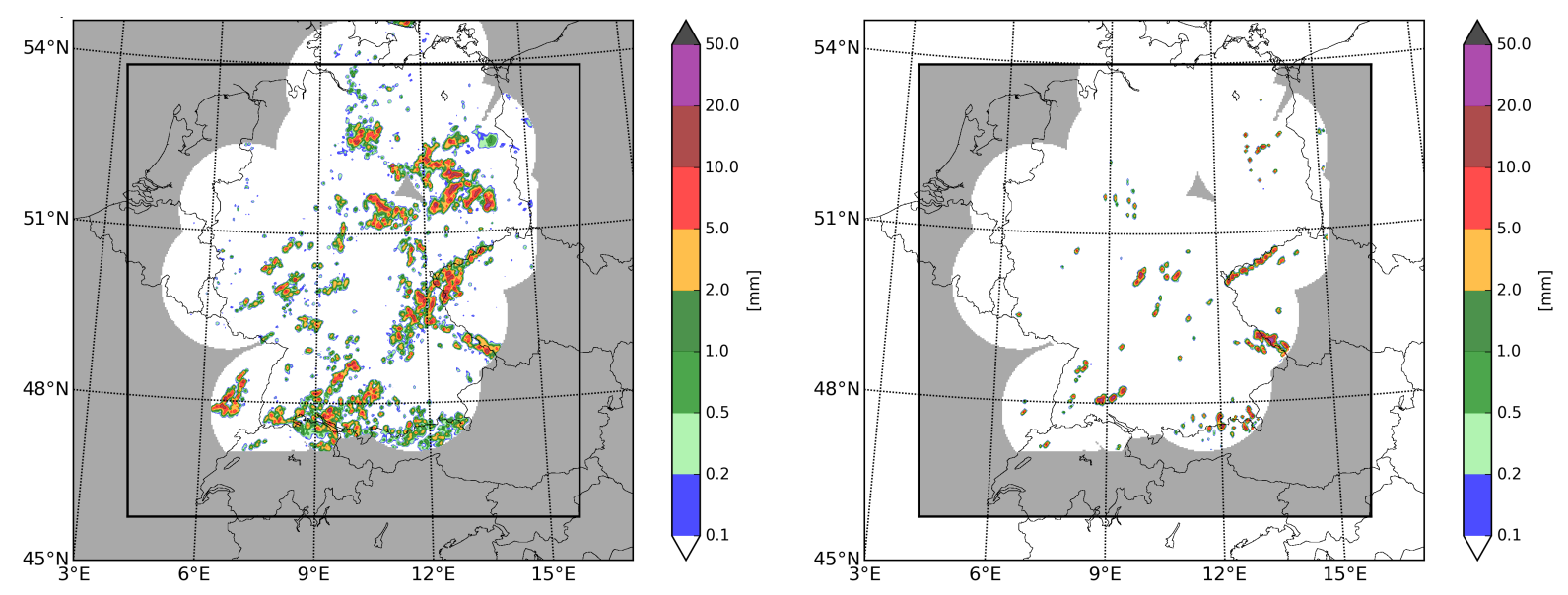


Fig. 1: Left: Observation of accumulated precipitation at 12 UTC for 1 July 2009. Right: like left but for COSMO-DE forecast.

Missing small-scale variability due to boundary layer processes is one reason.

Boundary layer processes - General

Several processes contribute to the variability in a convective boundary layer, eg. surface heating (sh), flow – subgrid-scale orography interaction (sso), cold pools (cp), mesoscale circulations (mc):

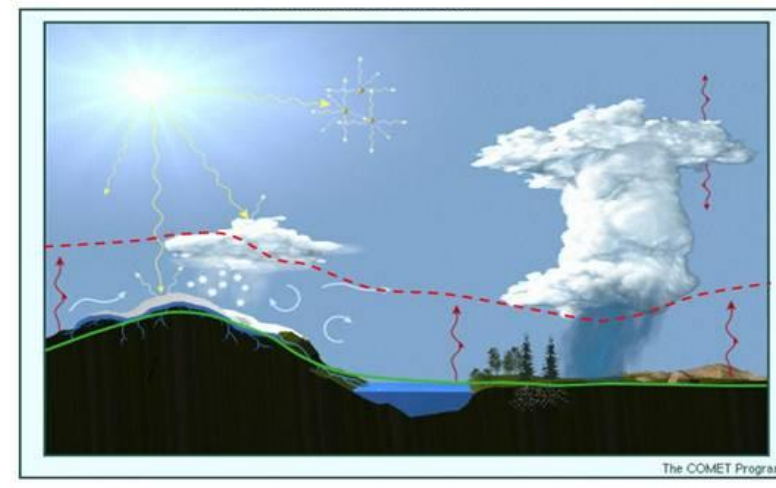


Fig. 2: Boundary layer processes creating small-scale variability.

Increasing the small-scale variability by stochastic perturbations representing boundary layer processes improves the precipitation forecast (Kober & Craig, 2016).

General equation for perturbations:

$$\left(\frac{\partial \Phi}{\partial t}\right)_{all}^{stoch} = \left(\frac{\partial \Phi}{\partial t}\right)_{sh}^{stoch} + \left(\frac{\partial \Phi}{\partial t}\right)_{sso}^{stoch} + \left(\frac{\partial \Phi}{\partial t}\right)_{cp}^{stoch} + \left(\frac{\partial \Phi}{\partial t}\right)_{mc}^{stoch}$$

An approach representing surface heating has shown improved forecast skill (see conference contribution of Stephan Rasp and Kober & Craig, 2016):

I. Basic principle

Heating of surface drives turbulence in boundary layer \Rightarrow relevant for initiation of convection

II. Mathematical formulation

Perturbation structure: $\left(\frac{\partial \Phi}{\partial t}\right)_{sh}^{stoch} = \frac{\partial \Phi}{\partial t} + \alpha_{sh} \cdot \eta_{sh} \cdot \langle \Phi^2 \rangle^{1/2} \Rightarrow$ tendencies of temperature T, vertical velocity w and moisture q perturbed

Φ : resolved variable T, w, q and fluxes $\langle \Phi^2 \rangle$ α_{sh} : scaling factor η_{sh} : random number field

Boundary layer processes - Subgrid-scale orography

Methods

I. Basic principle

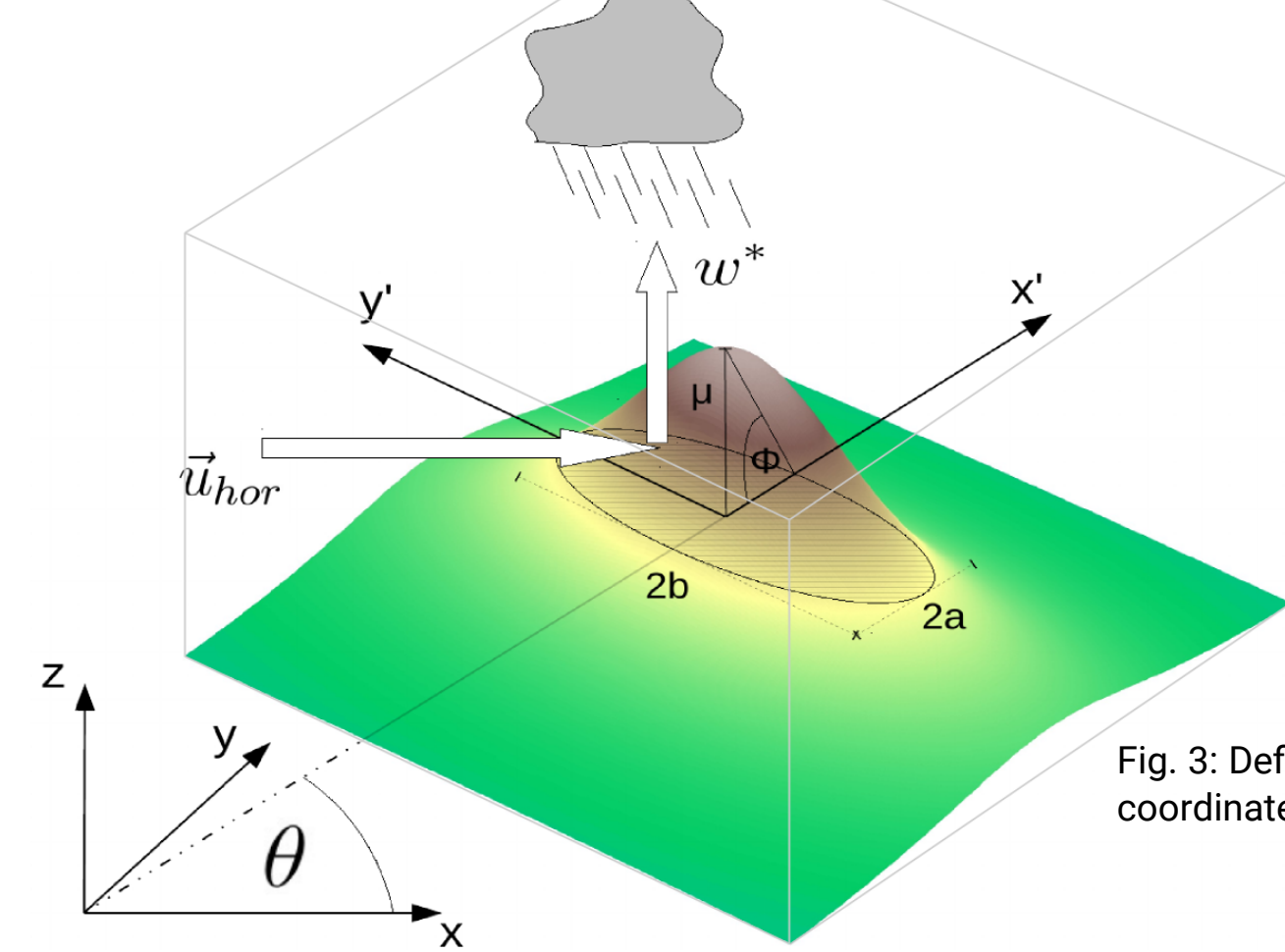


Fig. 3: Definition of the subgrid-scale orography parameters in rotated coordinates (x', y') , describing a bell-shaped mountain.

- Variability due to mechanical effect of subgrid-scale orography (SSO) on the atmospheric flow.
- Horizontal wind forces vertical motion leading to initiation of convection.
- COSMO-DE model configuration (2.8 km horizontal resolution).

II. Mathematical formulation

Perturbation structure: $\left(\frac{\partial \Phi}{\partial t}\right)_{sso}^{stoch} = \left(\frac{\partial w}{\partial t}\right)_{sso}^{stoch} = \frac{\partial w}{\partial t} + \frac{\alpha_{sso}}{dt} \cdot \eta_{sso} \cdot w^* \Rightarrow$ tendencies of vertical velocity w perturbed

w^* : forced vertical motion α_{sso} : scaling factor η_{sso} : random number field

Calculation of w^* based on internal gravity wave formalism for constant Brunt-Väisälä frequency N in an incompressible medium (Gill, 1982). w^* depends on SSO parameters (orientation θ , shape γ_{sso} , slope σ_{sso} , standard deviation of height μ_{sso}), horizontal wind (u', v') in the rotated SSO coordinates and stability N (see Baines & Palmer (1990) for details about SSO parameters):

$\omega^2 \leq N^2$ - vertical propagation possible:

$$w^* = w_0 \cdot \cos(kx + ly + mz - \omega t)$$

$\omega^2 > N^2$ - amplitude decays with height:

$$w^* = w_0 \cdot e^{-\gamma z} \cdot \cos(kx + ly - \omega t)$$

$$w_0 = w_0(k, l, u', v', \mu_{sso})$$

$$k = k(\sigma_{sso}, \mu_{sso})$$

$$l = l(\sigma_{sso}, \mu_{sso}, \gamma_{sso})$$

$$m = m(k, l, N^2)$$

$$\gamma^2 = -m^2$$

Results

I. Perturbations

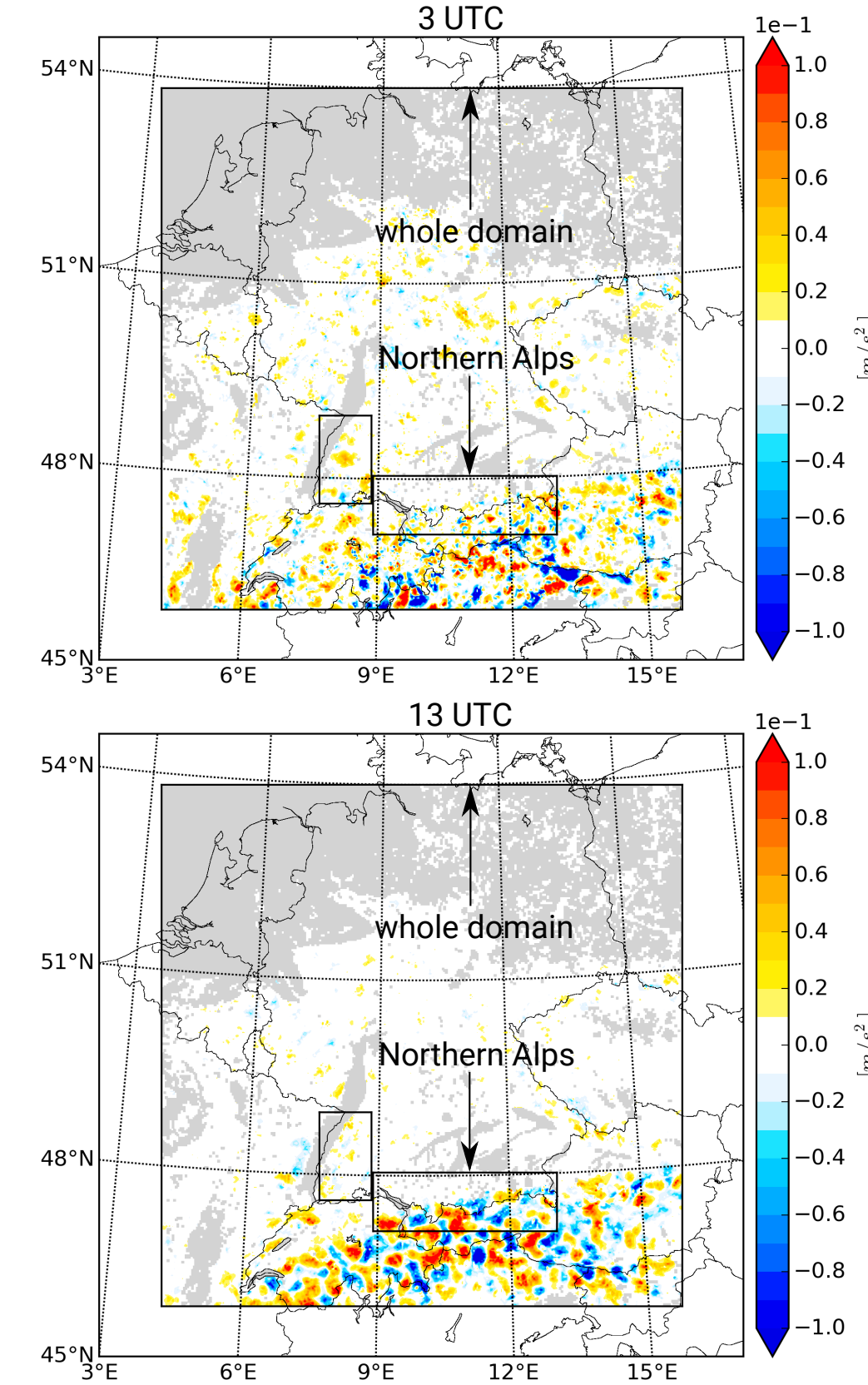


Fig. 4: Horizontal structure of perturbations $\frac{\partial \Phi}{\partial t} = \alpha_{sso} \cdot \eta_{sso} \cdot w^*$ for $\alpha = 1$ at model level 45 ($\approx 300m$ AGL) for 1 July 2009 (top: 3 UTC, bottom: 13 UTC). Grey shading marks areas where orographic variations are negligible.

- Perturbations larger over increased orographic variations due to scaling with slope parameter σ_{sso} .
- Diurnal variations small due to scaling with horizontal wind velocities u', v' .

II. Vertical velocity

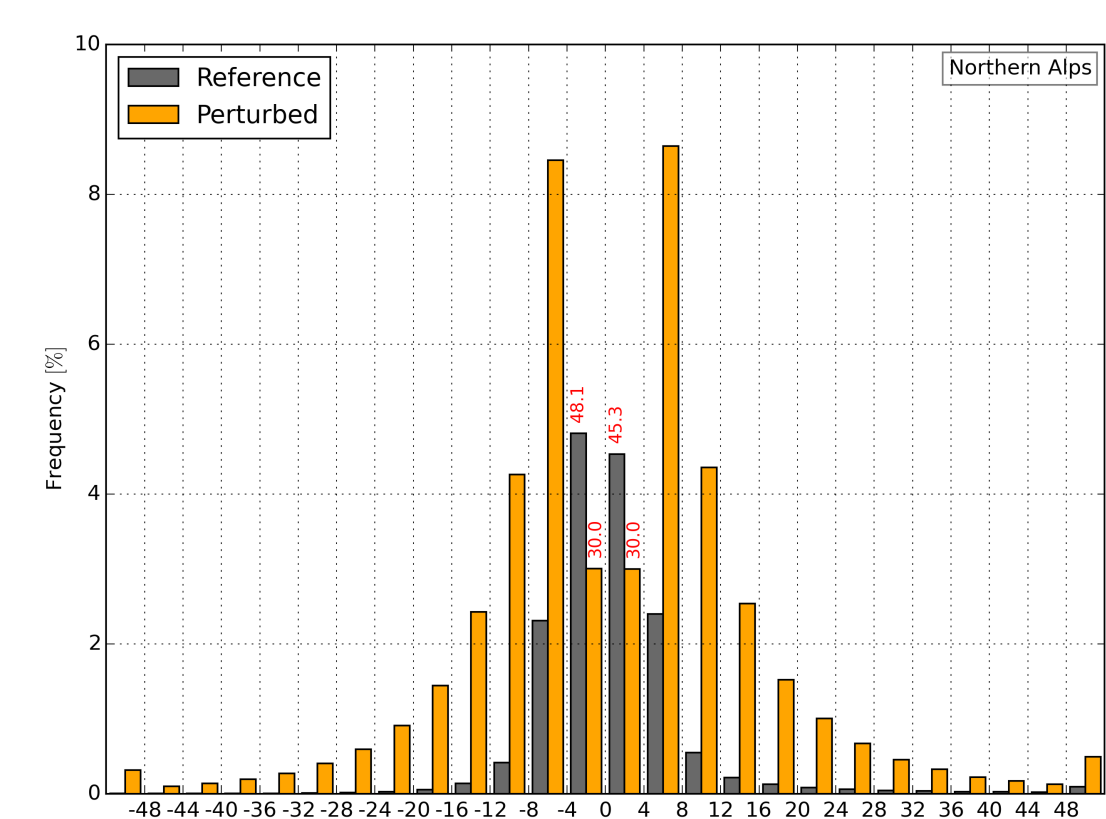


Fig. 5: Frequencies of vertically integrated vertical velocity w for 1 July 2009 between 01-23 UTC (Northern Alps). For better visualization the ranges around 0 m/s are divided by 10 and red numbers indicate the real frequencies.

\rightarrow Perturbations lead to increased variability of integrated vertical velocity with larger impact over mountainous areas

III. Specific humidity

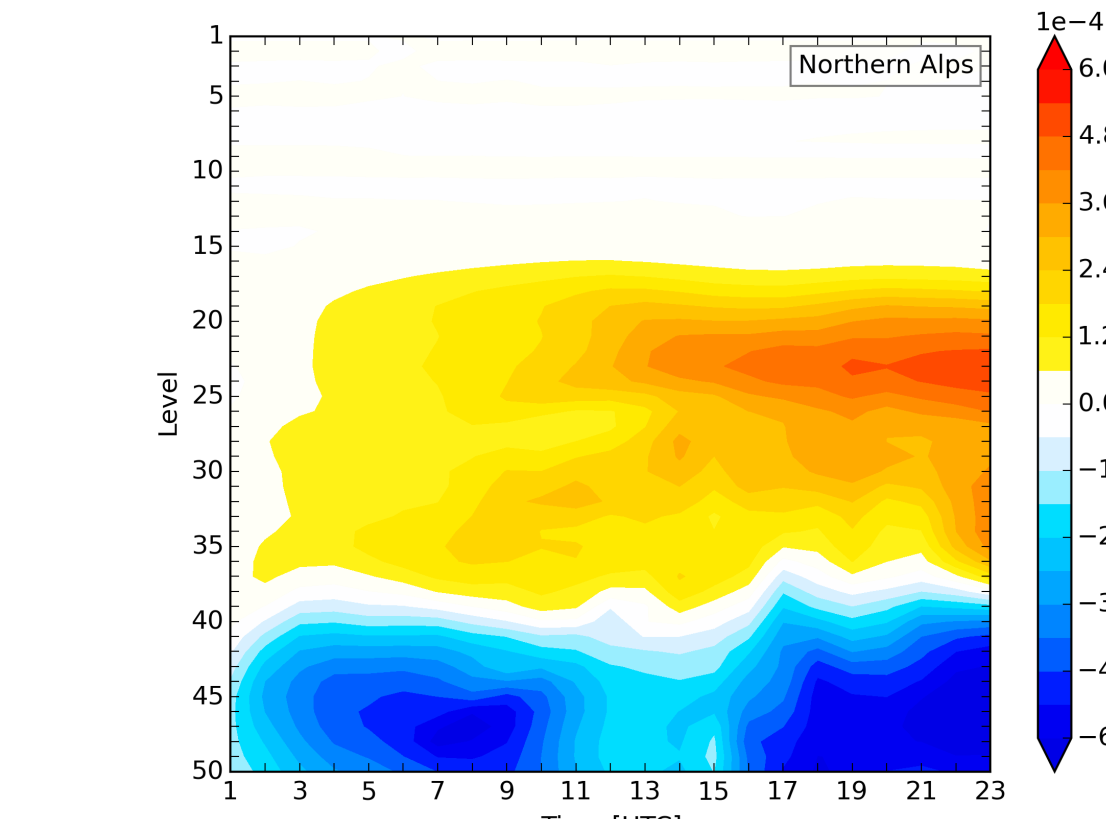
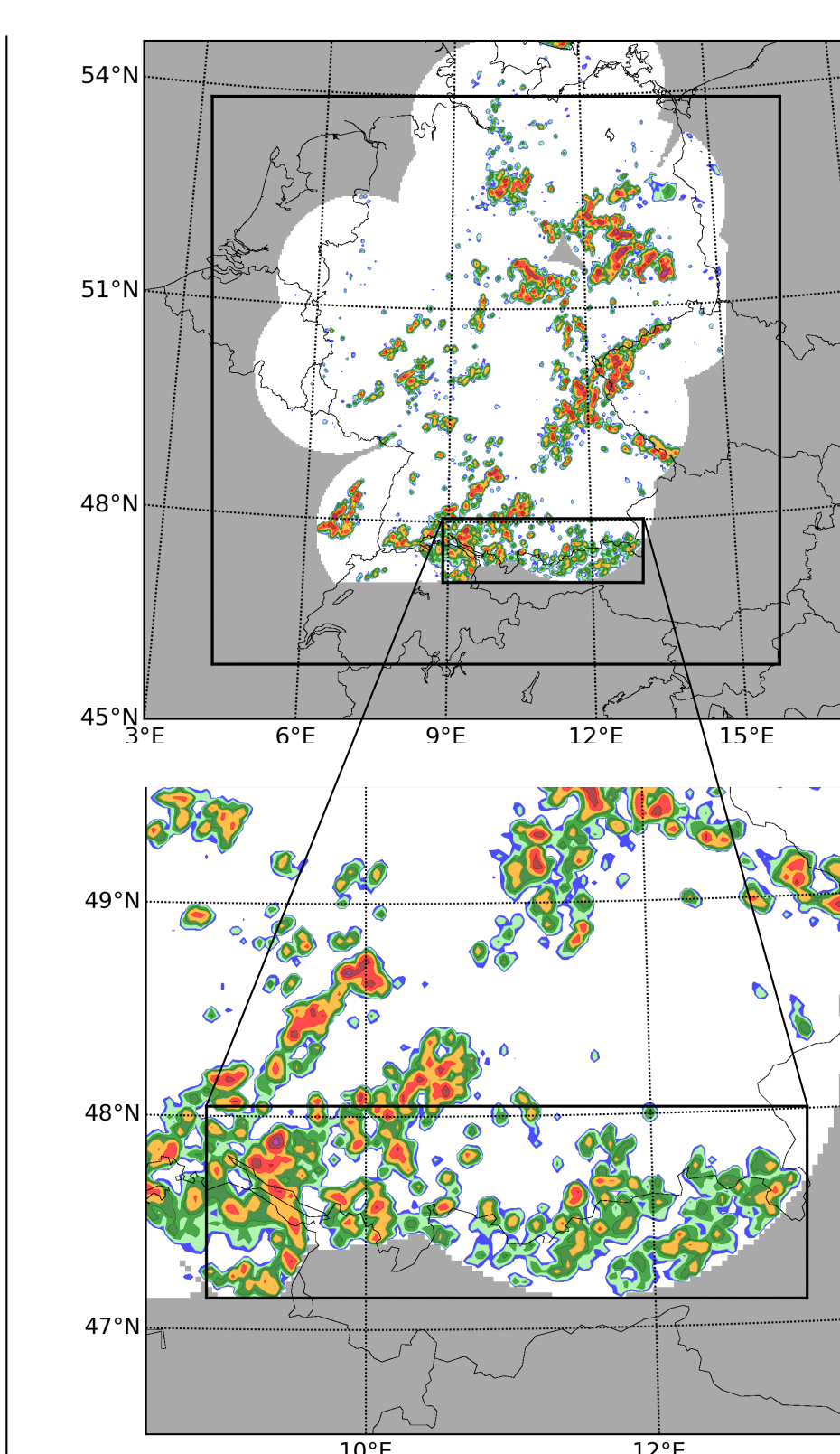


Fig. 6: Differences between a perturbed and reference simulation (perturbed - reference) of domain averaged specific humidity for 1 July 2009 (Northern Alps).

- Increased variability of vertical velocity enhances vertical transport of specific humidity.
- Drier boundary layer might suppress further initiation of convection.

IV. Precipitation



Weak synoptic forcing on 1 June 2014:

- Larger impact on precipitation compared to impact of scheme on 1 July 2009.
- Large variability among ensemble members.
- Root mean squared error (RMSE) slightly improved.

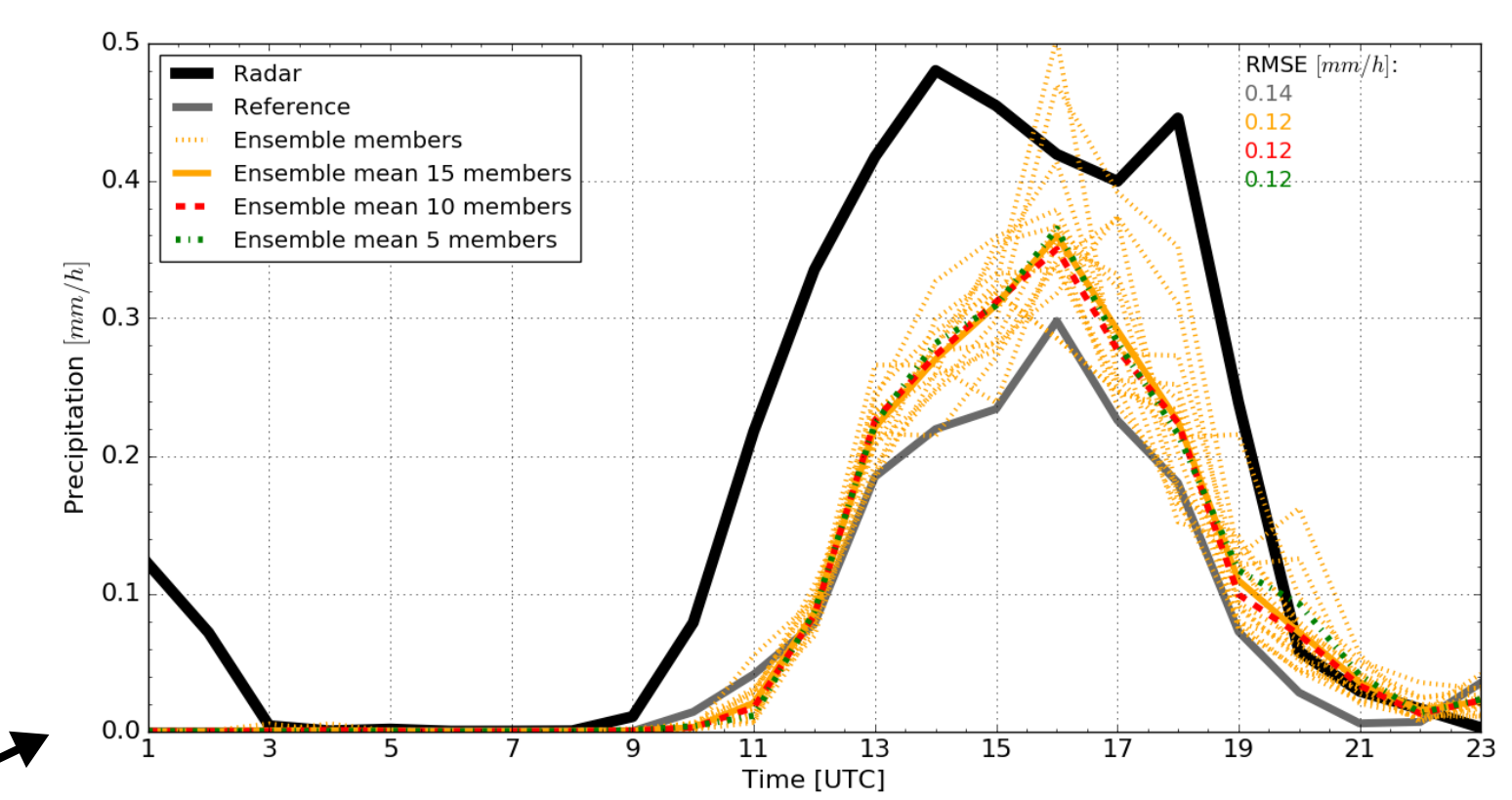


Fig. 7: Left top and bottom: Observation of accumulated precipitation at 12 UTC for 1 July 2009. Right top: Timeseries of domain average hourly precipitation rates for parts of the Northern Alps for 1 July 2009. Perturbations calculated with $\alpha = 1$.

Weak synoptic forcing on 1 July 2009:

- Larger impact of scheme over increased orographic variations.
- Ensemble with 10 members seems to be sufficient to capture mean precipitator rates.
- Root mean squared error (RMSE) slightly improved.
- Overall small impact on average precipitation rates compared to perturbation of other variables like temperature and moisture (see conference contribution Stephan Rasp and Kober & Craig, 2016) for 1 July 2009.

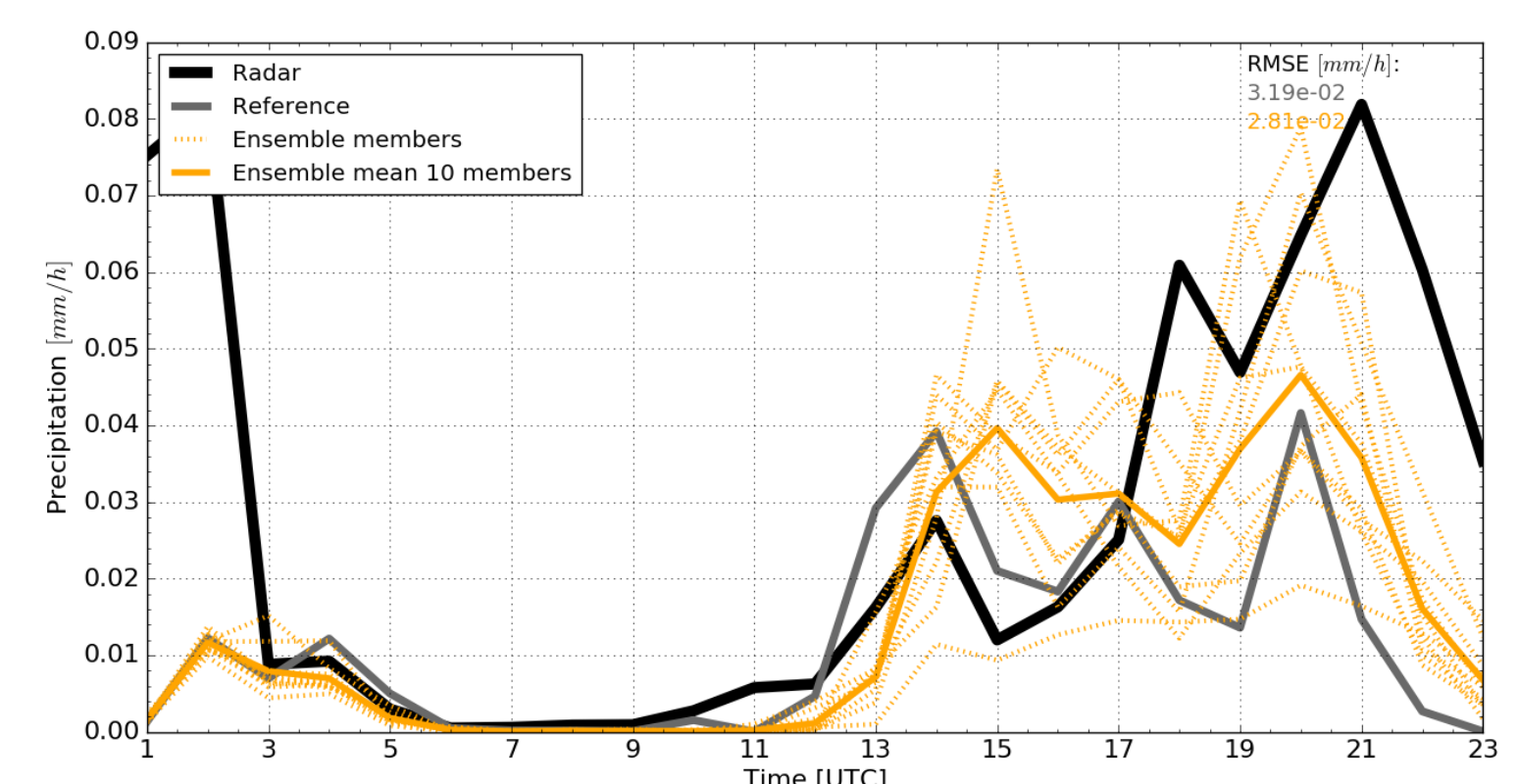


Fig. 8: Timeseries of domain average hourly precipitation rates for parts of the Northern Alps for 1 June 2014. Perturbations calculated with $\alpha = 1$.

Outlook

Develop and implement stochastic perturbation schemes, representing small-scale variability due to cold pools and mesoscale circulations:

Cold pools

I. Basic principle

Precipitating deep convective cells cool the air via evaporation which can lead to density currents at surface \Rightarrow alters the stability of the boundary layer and can trigger secondary cells

II. Mathematical formulation

Perturbation structure: $\left(\frac{\partial \Phi}{\partial t}\right)_{cp}^{stoch} = \left(\frac{\partial q}{\partial t}\right)_{cp}^{stoch} = \frac{\partial q}{\partial t} + \alpha_{cp} \cdot \eta_{cp} \cdot f(vel, lt) \Rightarrow$ tendencies of moisture q perturbed

α_{cp} : scaling factor η_{cp} : random number field vel : propagation velocity of cold pool lt : lifetime of cold pool

Mesoscale circulations

I. Basic principle

Mountain circulations due to differential heating and other processes can lead to convergence of air \Rightarrow relevant for initiation of convection

II. Mathematical formulation

Perturbation structure: $\left(\frac{\partial \Phi}{\partial t}\right)_{mc}^{stoch} = \frac{\partial \Phi}{\partial t} + \alpha_{mc} \cdot \eta_{mc} \cdot f(h, sso) \cdot f(\langle \Phi^2 \rangle) \Rightarrow$ tendencies of temperature T, vertical velocity w and moisture q perturbed

Φ : resolved variable T, w, q and fluxes $\langle \Phi^2 \rangle$ α_{mc} : scaling factor η_{mc} : random number field h : resolved orography sso : subgrid-scale orography

References:

- Kober, K. and Craig, G. C. (2016). *Stochastic boundary layer perturbations to represent uncertainty in convective initiation*. Journ. of the Atm. Sci. In revision.
- Baines, P. G. and Palmer, T. (1990). *Rationale for a new physically-based parametrization of subgrid-scale orographic effects*. ECMWF.
- Gill, A. E. (1982). *Atmosphere-Ocean Dynamics*. Academic Press.